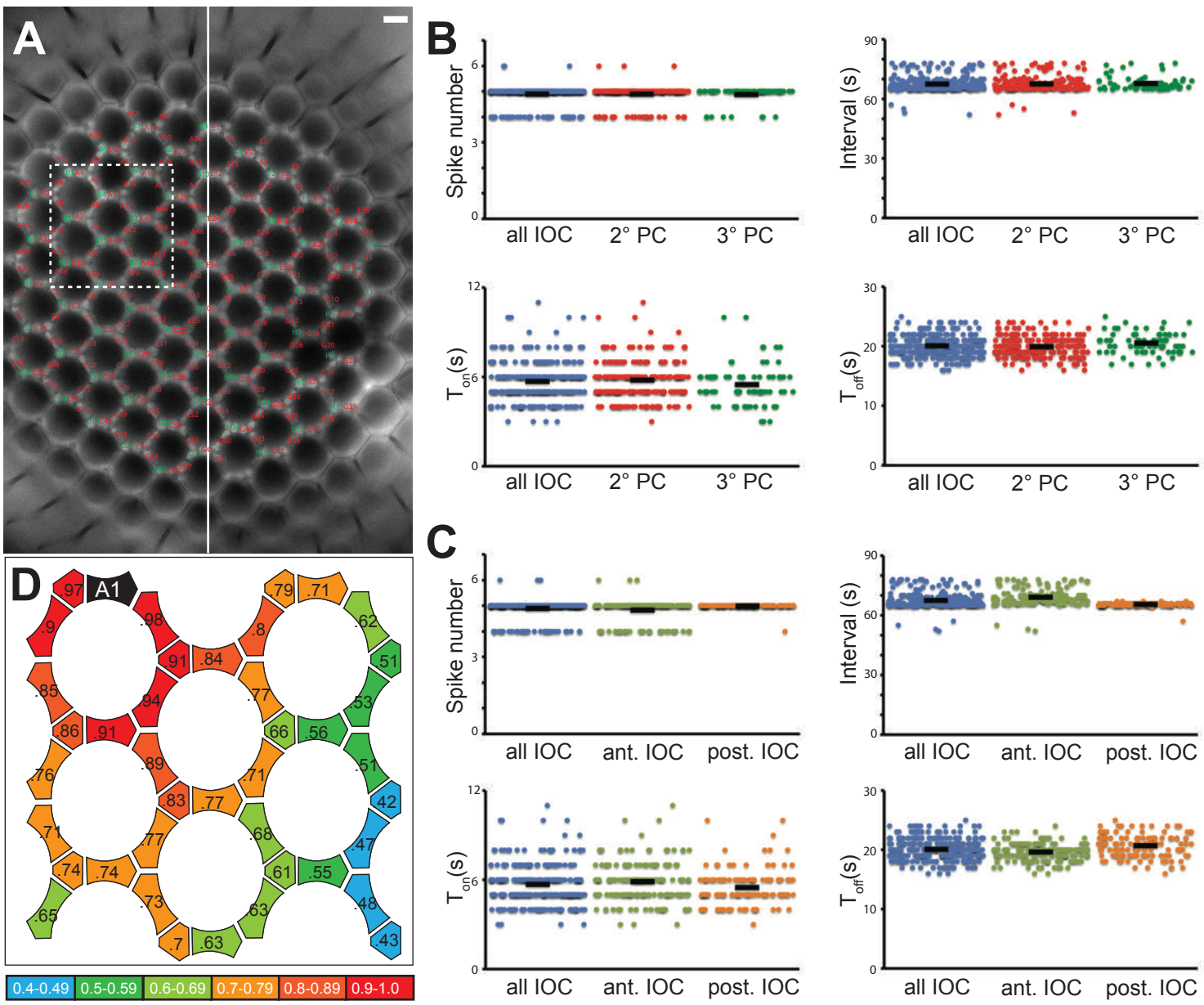

Fig. S1. IOC Ca^{2+} transients are similar across the retina. (A) A micrograph of *IGMR>GCaMP6/+* retina showing secondary (green) and tertiary (red) pigment cells labeled for quantitative analysis. A white line artificially demarcates the anterior and posterior halves. Scale bar=10μm. (B) Scatter plots of spike characteristics from IOCs (n=273 cells, blue dots), secondary (n=204 cells, red dots), and tertiary (n=69 cells, green dots) pigment cells from this recording. Dots represent the numbers (spike numbers, interval averages, and T_{ON} and T_{OFF} averages) obtained from individual cells, and averages from cell populations are indicated by black bars. (C) Comparison of IOC Ca^{2+} spike parameters from the anterior (n=118 cells, light green dots) and posterior (n=155 cells, orange dots) halves. Averages from different halves are indicated by black bars. (D) A schematic map showing pair-wise Pearson correlation analysis performed on numeric series generated from GCaMP6m intensities over time with cell A1. Region containing analyzed clusters corresponds to the dashed box in A. The cells closest to A1 exhibit higher correlations than those farther away.

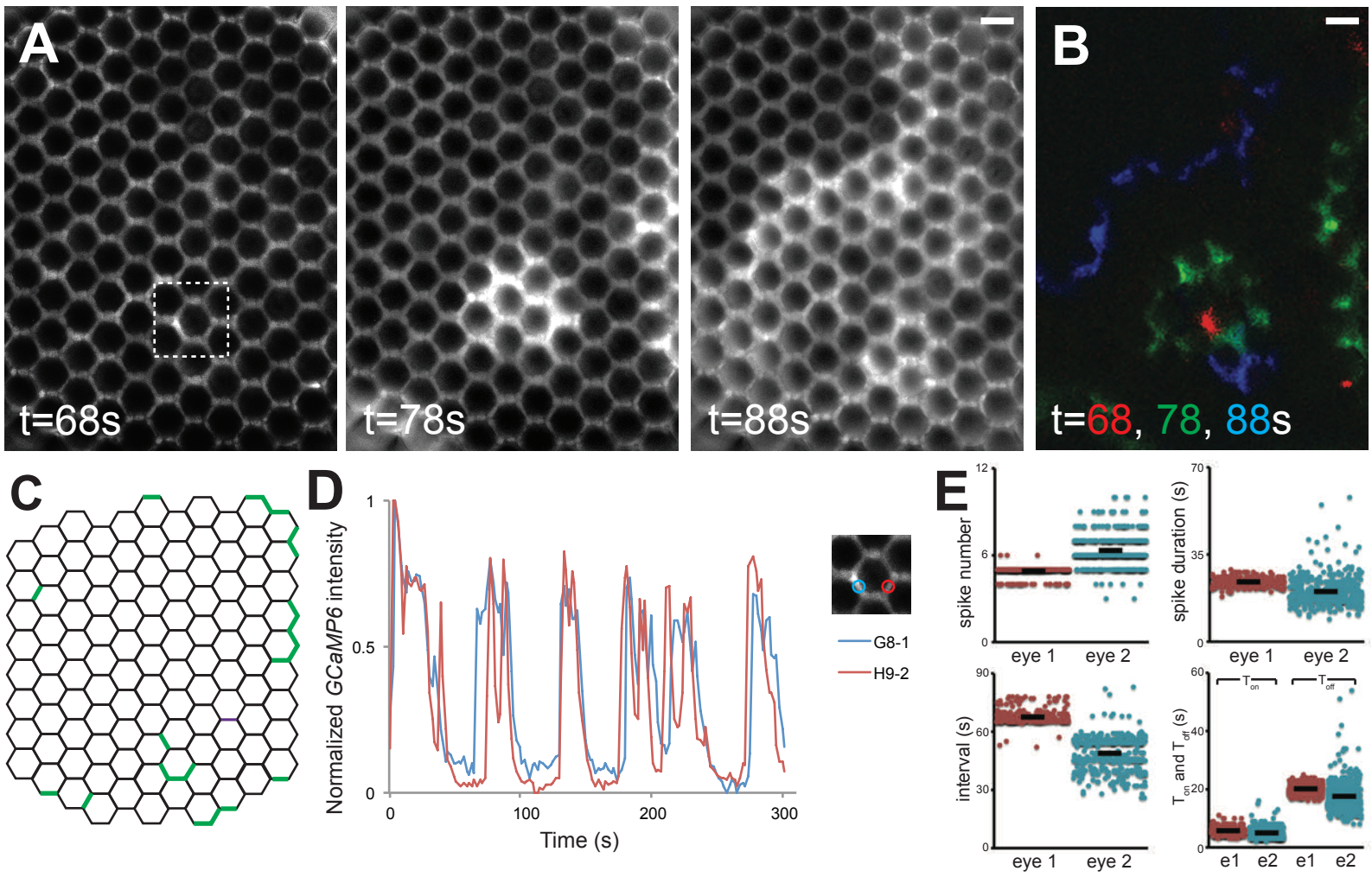

Fig. S2. Comparison of IOC waves from two independent eyes. (A) A micrograph montage of 10s intervals showing a Ca^{2+} wave initiated in the ventral region (dashed box) of a young *IGMR>GCaMP6m* retina at t=68s. Scale bar=10μm. (B) An image overlaying three wave fronts at t=68s (red), 78s (green), and 88s (blue) respectively. This IOC wave is the same one shown in A. At t=78 sec, a distinct wave front approaches from the anterior edge. (C) A schematic representation of the IOC wave origins, each denoted with a green line. Comparing to the movie shown in Fig. 2, this recording is noisier with more “flickering”, and only those resulted in waves are indicated. (D) Plot of normalized GCaMP6m intensity ((F-Fmin)/(Fmax-Fmin)) over time showing the regular Ca2+ oscillation in 2 secondary pigments cells (G8-1 and H9-2), selected from the dashed box in A. (E) Scatter plots comparing IOC Ca2+ spike characteristics from two independent young IGMR>GCaMP6m retinas. Eye 1 corresponds to the retina shown in Fig. 2 (n=273 cells, dark red dots) and Eye 2 (n=474 cells, light blue dots) is the retina shown in this figure. Dots represent the numbers from individual cells, and averages from IOCs of different eyes are indicated by black bars.

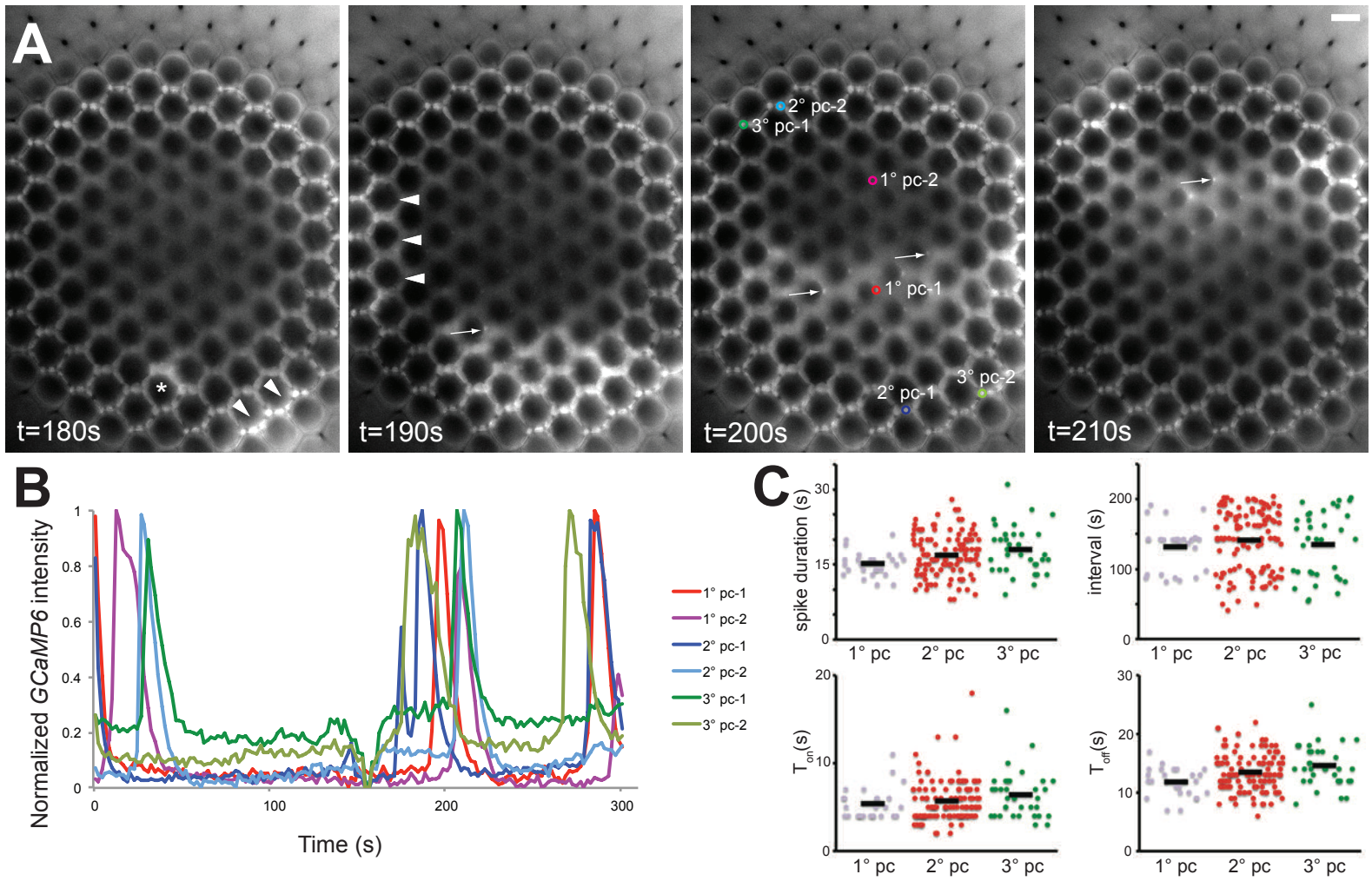

Fig. S3. IOC waves propagate through primary, secondary, and tertiary pigment cells. (A) A young adult retina showing *GCaMP6m* signals from all three pigment cell types in different regions of the eye. Because of the retinal curvature, Ca^{2+} transients from secondary and tertiary pigment cells are readily recognized around the retinal periphery, whereas signals from the nuclei of anterior primary pigment cells in the central region are seen (arrows). In primary pigment cells, *GCaMP6m* signals in the nuclei are more prominent because of the quenching of cytoplasmic *GCaMP6m* fluorescence by pigment granules. The nuclei from the posterior primary pigment cells are not visible due to the angle of specimen preparation. At t=180s, wave initiations were seen at the anterior-ventral edge (arrowheads) and in nearby internal IOC cells (asterisk). At t=190s, another wave front was seen at the posterior edge (arrowheads). These waves then merged and moved dorsally across the *GCaMP6m* retina through all three pigment cell types. (B) Plot of normalized *GCaMP6m* intensity ($(F-F_{min})/(F_{max}-F_{min})$) over time showing the Ca2+ oscillation in two primary (red and magenta lines), two secondary (blue and light blue), and two tertiary (green and light green) cells. The line colors correspond to color circles (selected cells) in A. The dip in GCaMP6m intensity around t=160s was caused by a sudden movement of the specimen. (C) Scatter plots comparing spike characteristics (duration, interval, Ton, and Toff) between primary (n=26 cells, gray dots), secondary (n=115 cells, red dots), and tertiary (n=35 cells, green dots) pigment cells of this recording. Averages of different cell types are indicated by black bars.

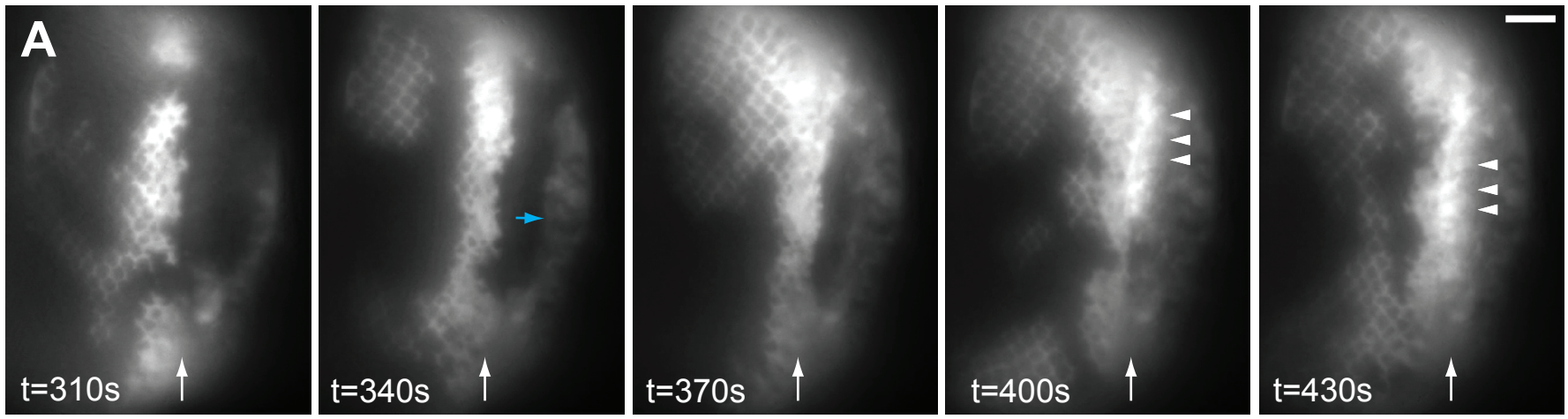

Fig. S4. Ca^{2+} waves are present in larval eye discs. (A) A micrograph montage of an *ey-GAL4; UAS-GCaMP6m* eye disc in 30s intervals, showing the presence of Ca^{2+} waves behind and ahead of the furrow (arrows). Instead of *IGMR-GAL4*, the larval eye disc was recorded with *ey-GAL4* to detect Ca^{2+} activities in cells anterior and posterior to the furrow. Ahead of the furrow, Ca^{2+} waves are present, but less frequent, and an example is shown initiating from the anterior edge at t=340s (blue arrow), reaching the furrow at ~400s. At the furrow, when cells experience Ca^{2+} spikes, high GCaMP6m signals are seen in regularly spaced cell clusters (arrowheads). Posterior to the furrow, Ca^{2+} waves are frequent with higher GCaMP6m signals in pre-IOCs, resulting in a honeycomb-like appearance. Scale bar=40μm.

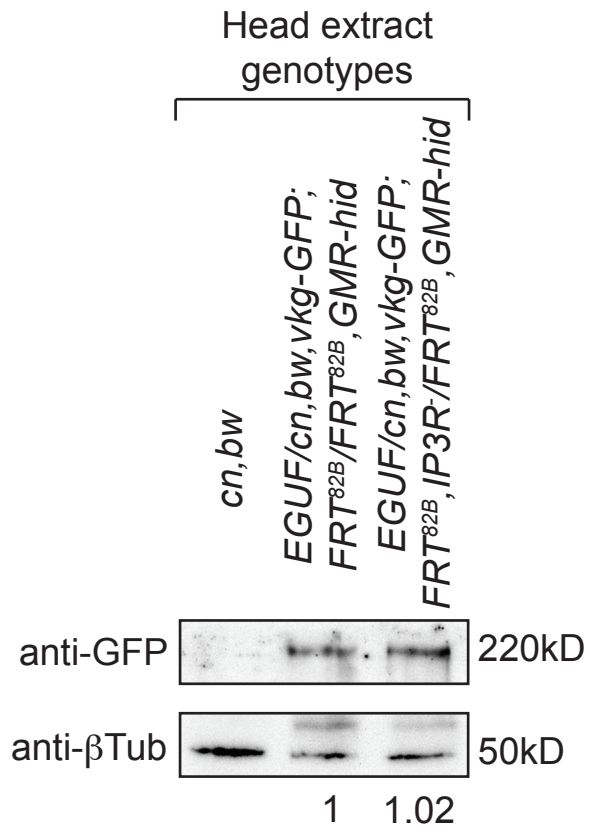

Fig. S5. vkg synthesis is unaffected in *IP3R*$^{-}$ retina. Western blot of total head lysates from *cn, bw* (lane 1), *ey-GAL4, UAS-FLP/vkg::GFP; FRT*^{82B}*/FRT*^{82B}*, GMR-hid* (lane 2), and *ey-GAL4, UAS-FLP/vkg::GFP; FRT*^{82B}*, l(3)itpr*$^{90B.0}$*/FRT*^{82B}*, GMR-hid* (lane 3). The vkg::GFP proteins, absent in cn, bw extract, are detected by anti-GFP antibody, and the β-tubulin bands serve as loading controls. The GFP/β-tubulin band intensity ratios are determined with ImageJ.

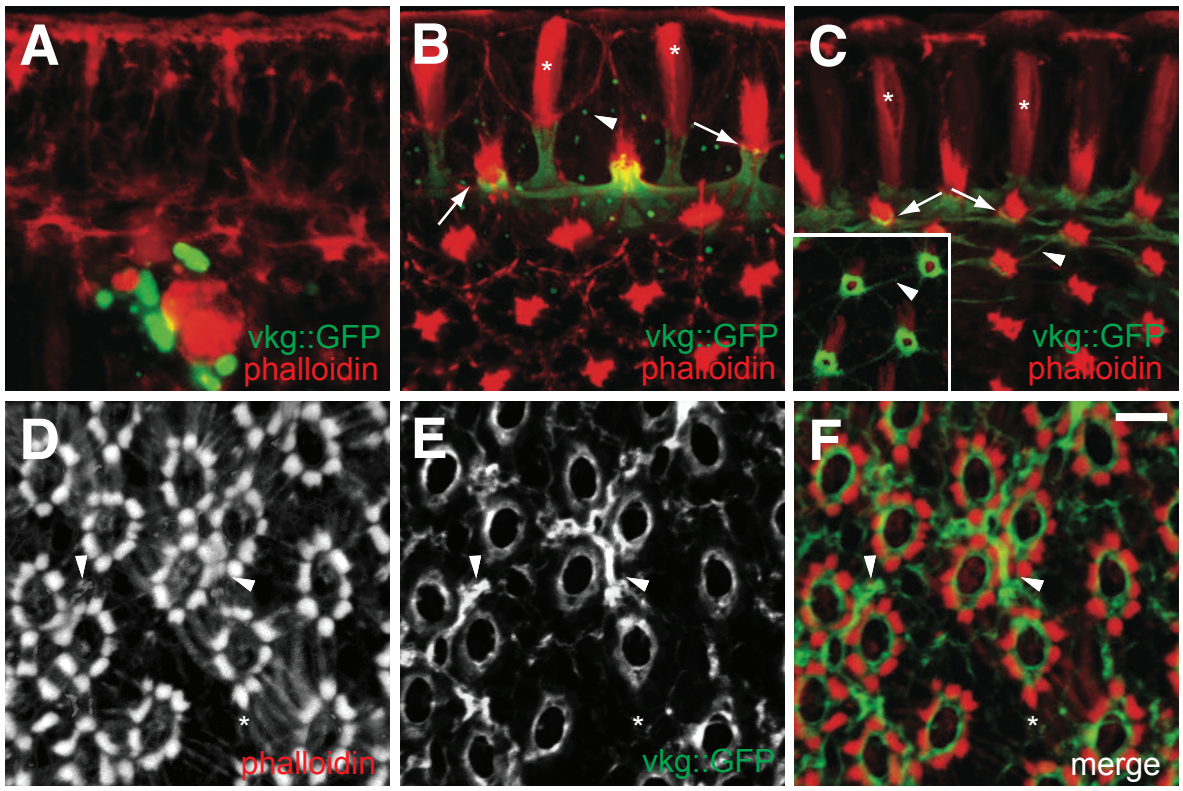

Fig. S6. The formation of grommets and ridges during pupal development. A-F) Snapshots of 3D rendering of confocal sections of *cn, bw, vkg::GFP* pupal retinas stained with phalloidin (red). (A) Prior to rhabdomere extension (at ~30% pupal development), unorganized vkg-positive structures are seen underneath the retina. (B) As the rhabdomeres (asterisks) are in the midst of extending throughout the depth of the retina (at ~45% pupal development), vkg-positive cylindrical structures rise from the basement membrane to interface with the growing rhabdomeres. At this stage, the photoreceptor cell cortex, revealed by phalloidin staining, and vkg-positive cylinder assume the appearance of a wineglass (with photoreceptor cell cortex being the “bowl” and vkg cylinder being the “stem”). The junctures between the rhabdomeres and vkg::GFP stems constitute the future grommets (arrows). In addition, vkg-positive puncta are seen inside the IOCs (arrowheads), suggesting that these cells deposit the ECM into the basement membrane. (C) At the completion of rhabdomere extension (at ~60% pupal development), elevated vkg::GFP signal labels the grommets (arrows, inset) and the IOC basal cell contacts at the retinal floor (arrowheads). A bottom view of a pupal eye at a similar stage as in (C) is shown in the inset. (D-F) At a later stage, the presence of vkg ridges correlates with the extent of actin stress fiber contraction, which varies across this retina. In regions where the stress fibers have contracted, the vkg ridges are prominent (arrowhead). In contrast, vkg ridges are reduced in regions where the stress fibers are extended (asterisk). Scale bar=10μm.

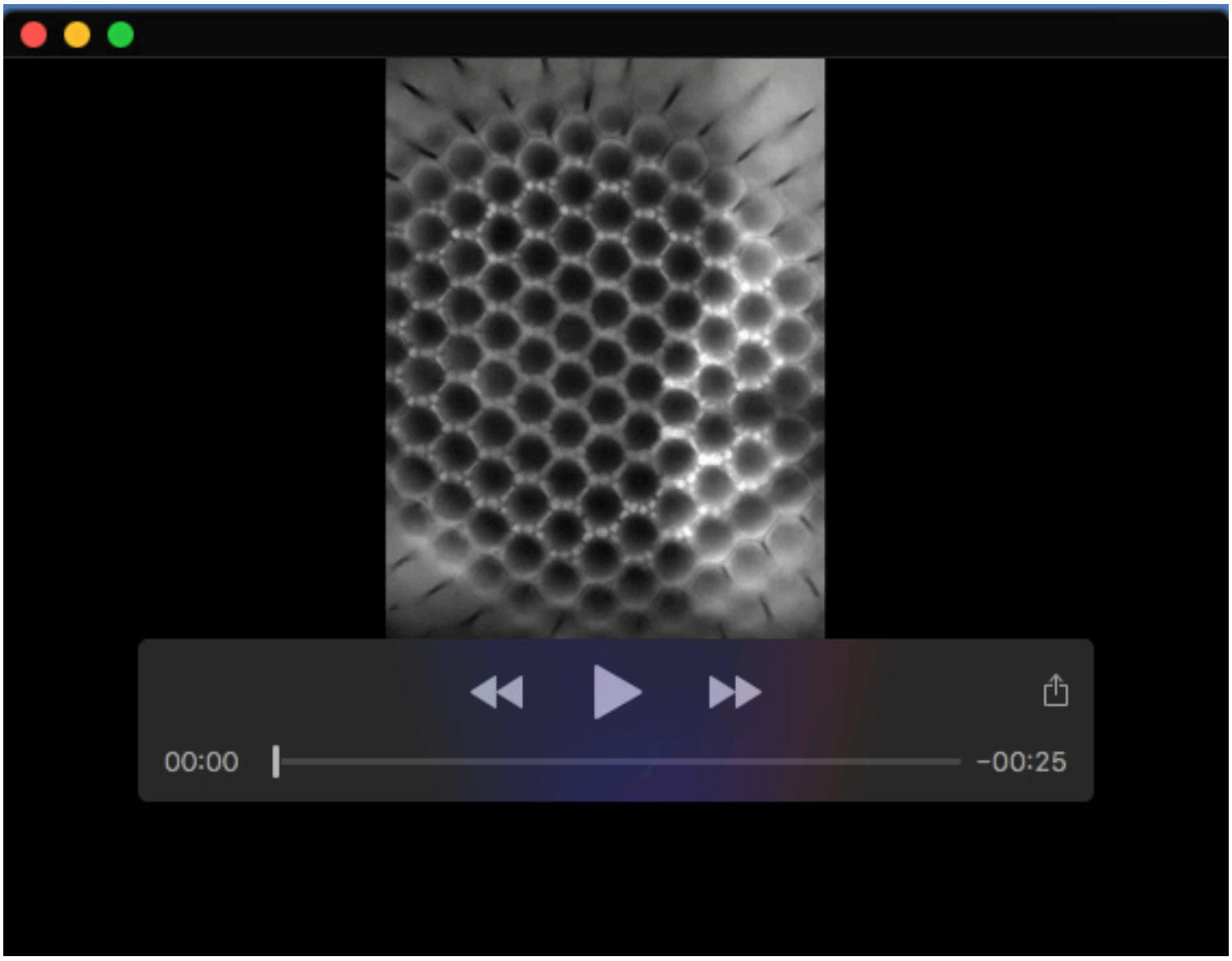

Movie 1. Young *lGMR>GCaMP6m/+* adult retina at a distal plane (Fig. 2), revealing Ca^{2+} waves in IOCs.

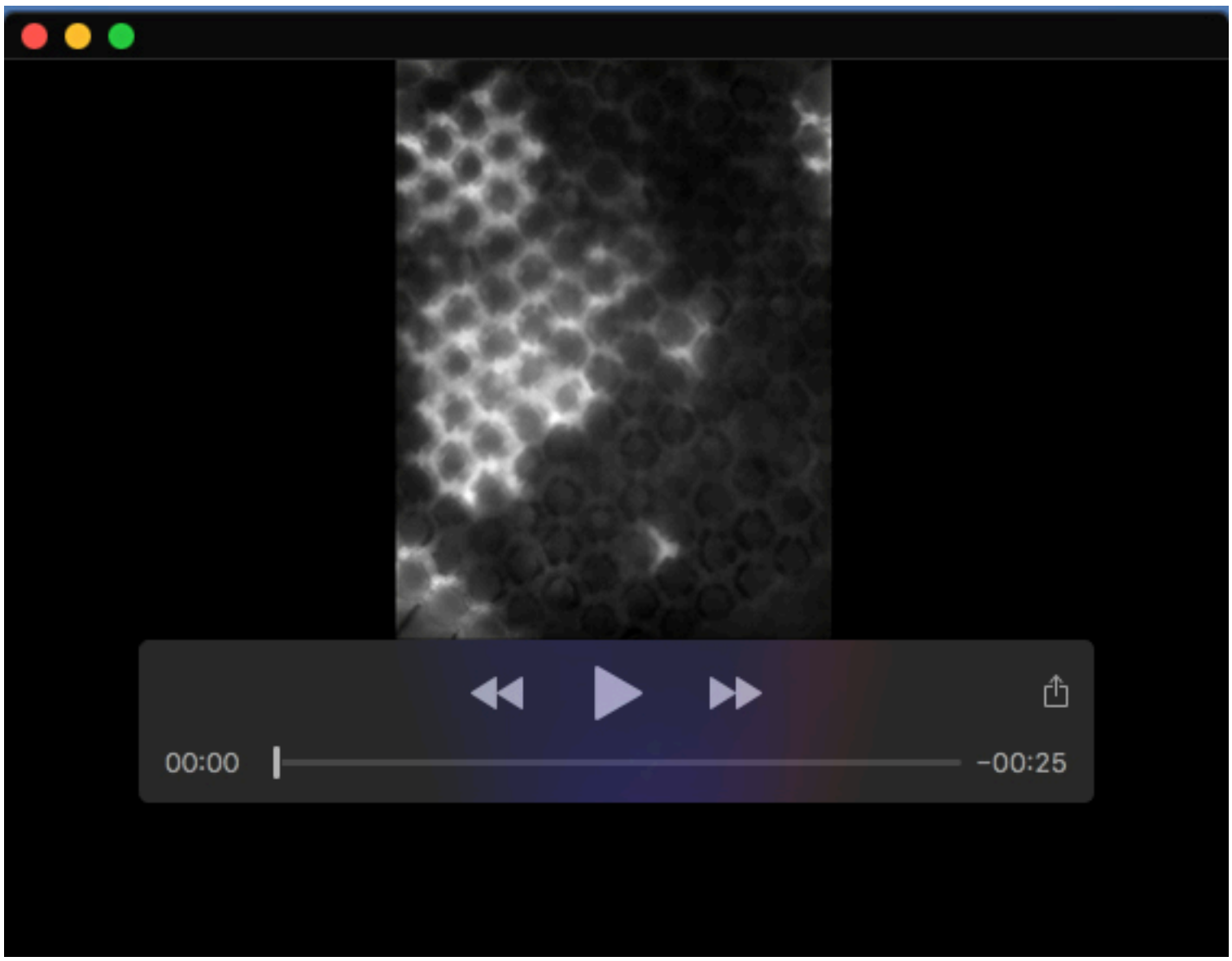

Movie 2. Young *IGMR>GCaMP6m/+* adult retina at a proximal plane (Fig. 3), showing Ca2+ waves in primary pigment cells.

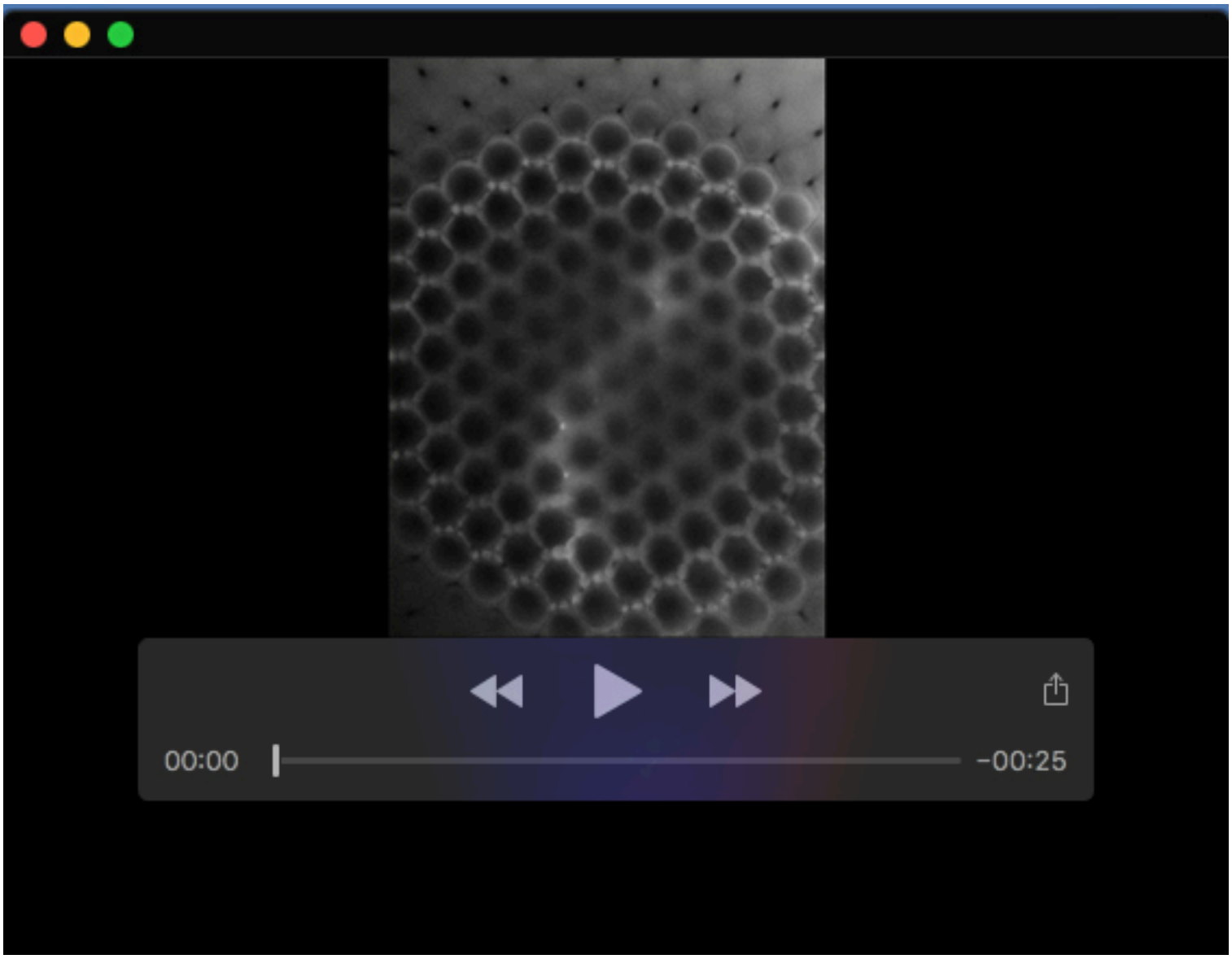

Movie 3. Young lGMR>GCaMP6m/+ adult retina at a proximal plane (Fig. S3), showing Ca2+ waves in primary pigment cells in the center and IOC waves in the peripheryof the eye.

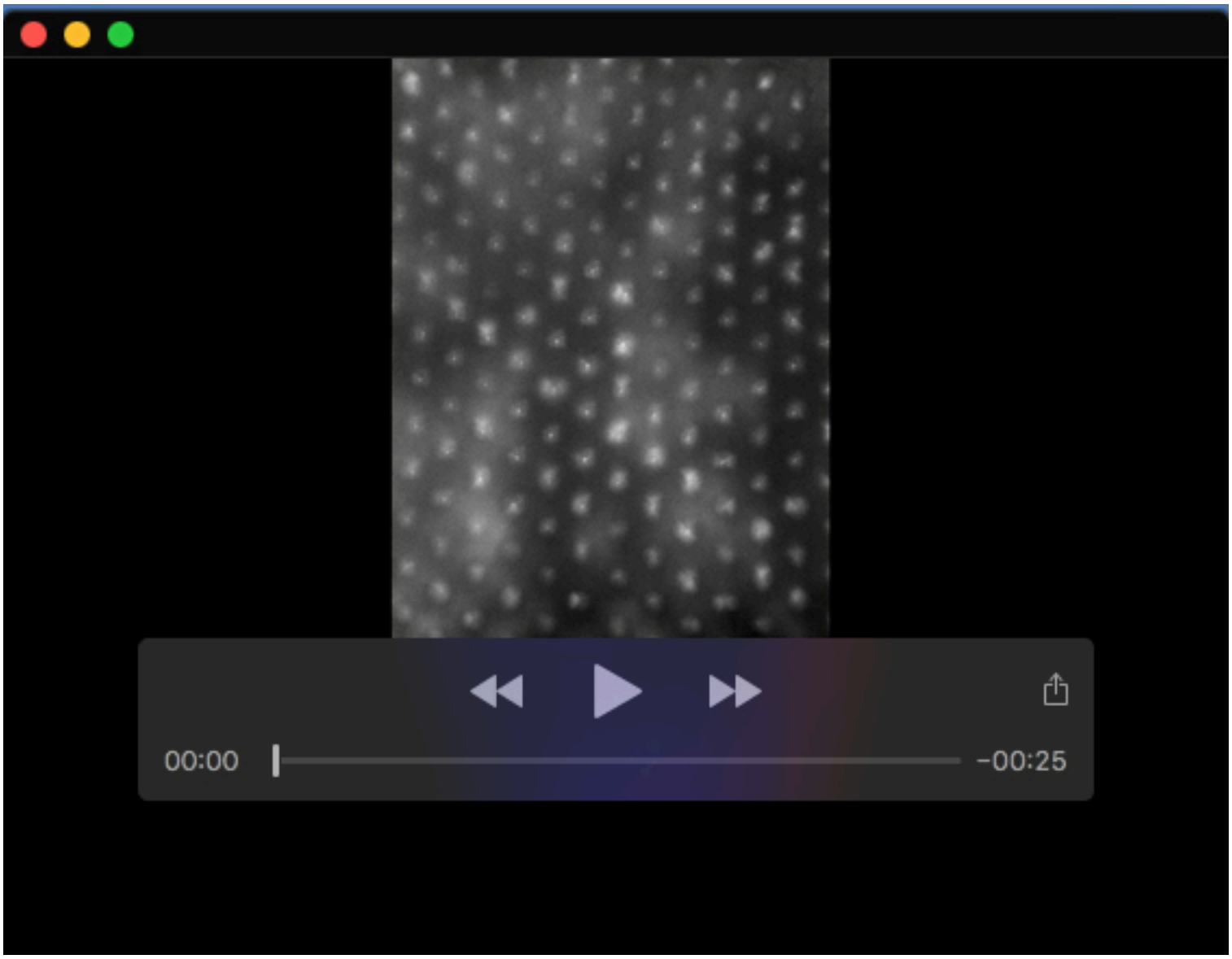

Movie 4. Young *IGMR>GCaMP6m/+* adult retina at a proximal plane (Fig. 4), showing Ca2+ activities in cone cells.

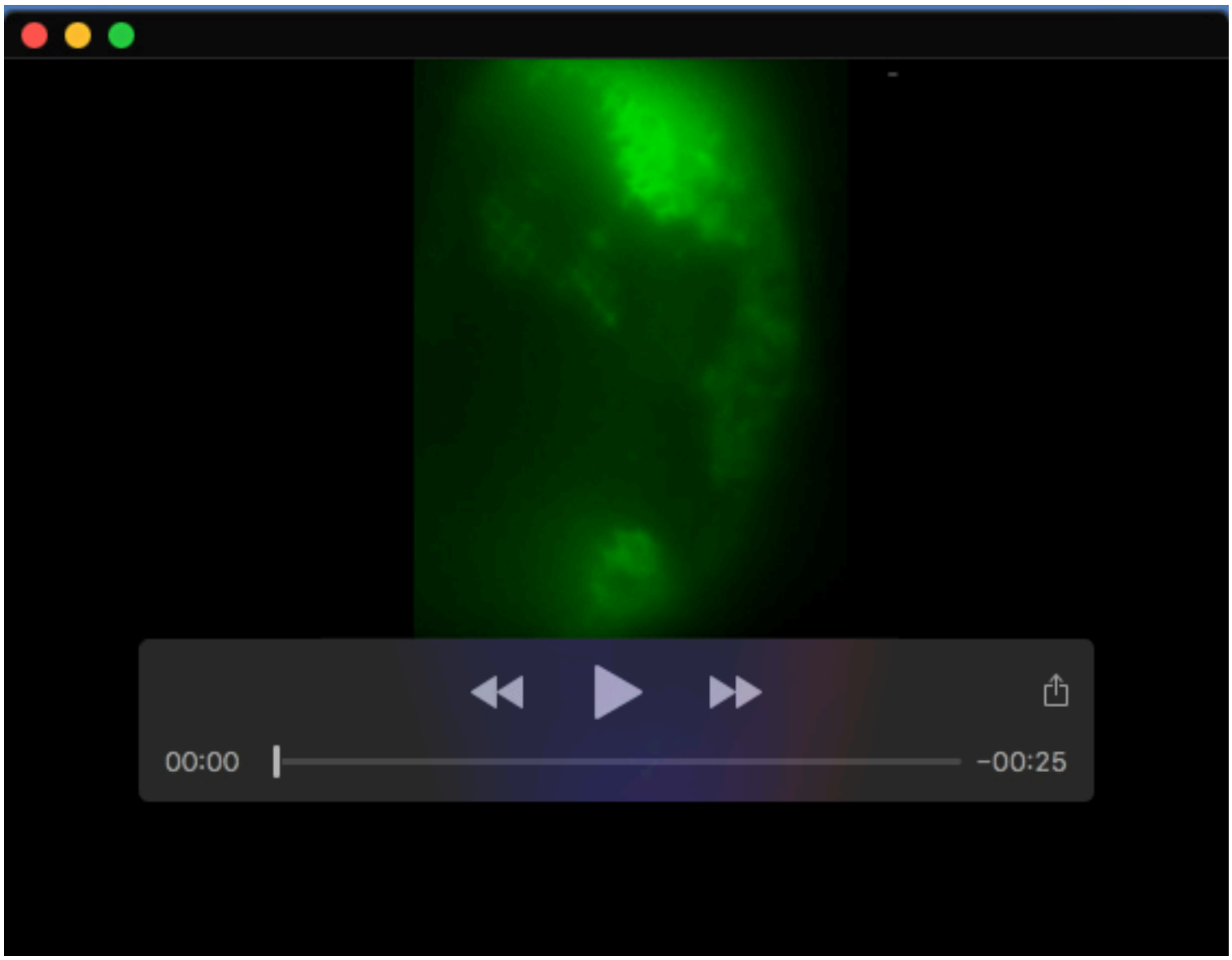

Movie 5. *ey>GCaMP6m/+* larval eye disc (Fig. S4). This time lapse was captured for a 10-minute duration.

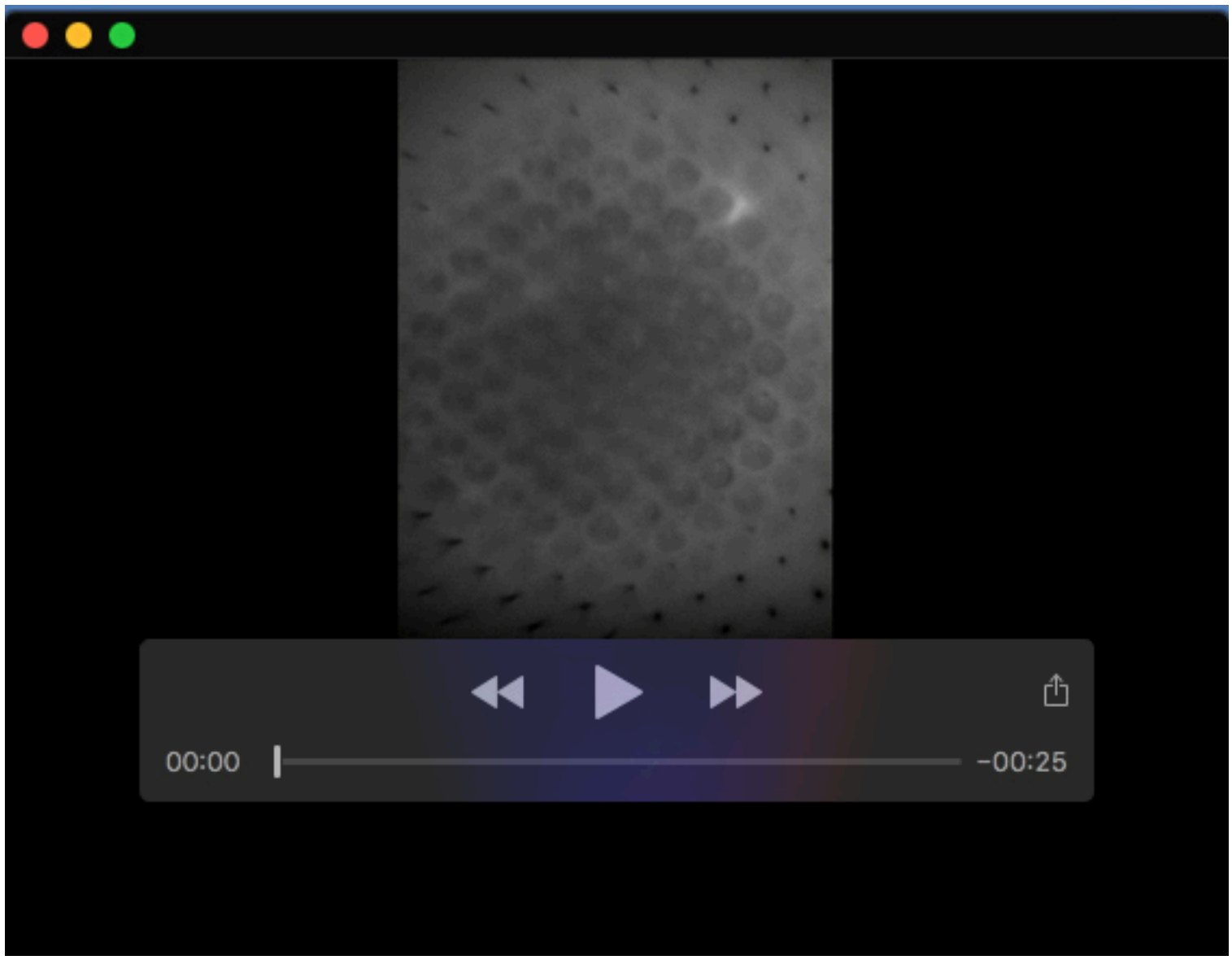

Movie 6. *lGMR>GCaMP6m/+* pupal retina at approximately P12 stage (Fig. 5).

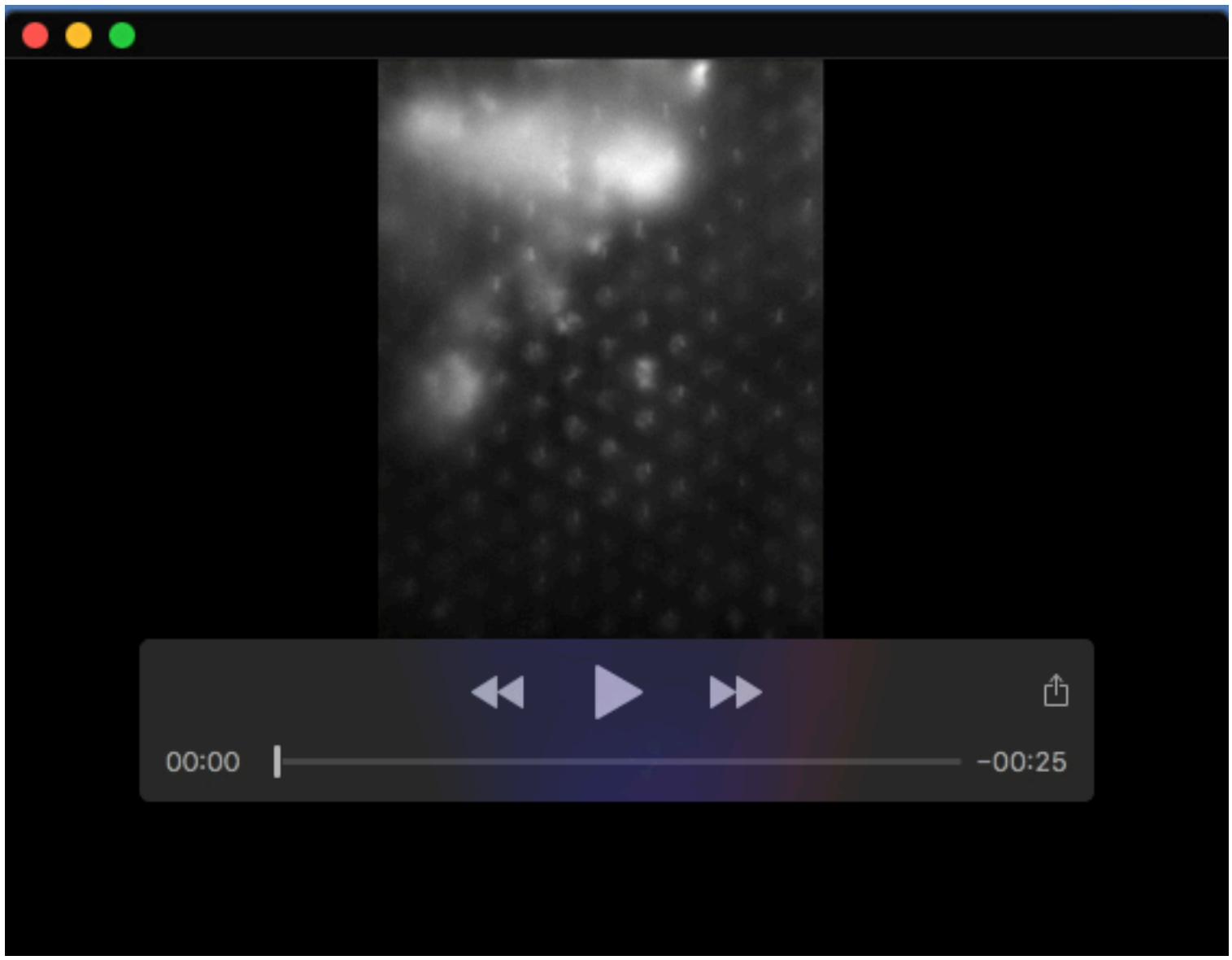

Movie 7. The same *IGMR>GCaMP6m/+* pupal retina from Movie 6 imaged one day later (Fig. 5).

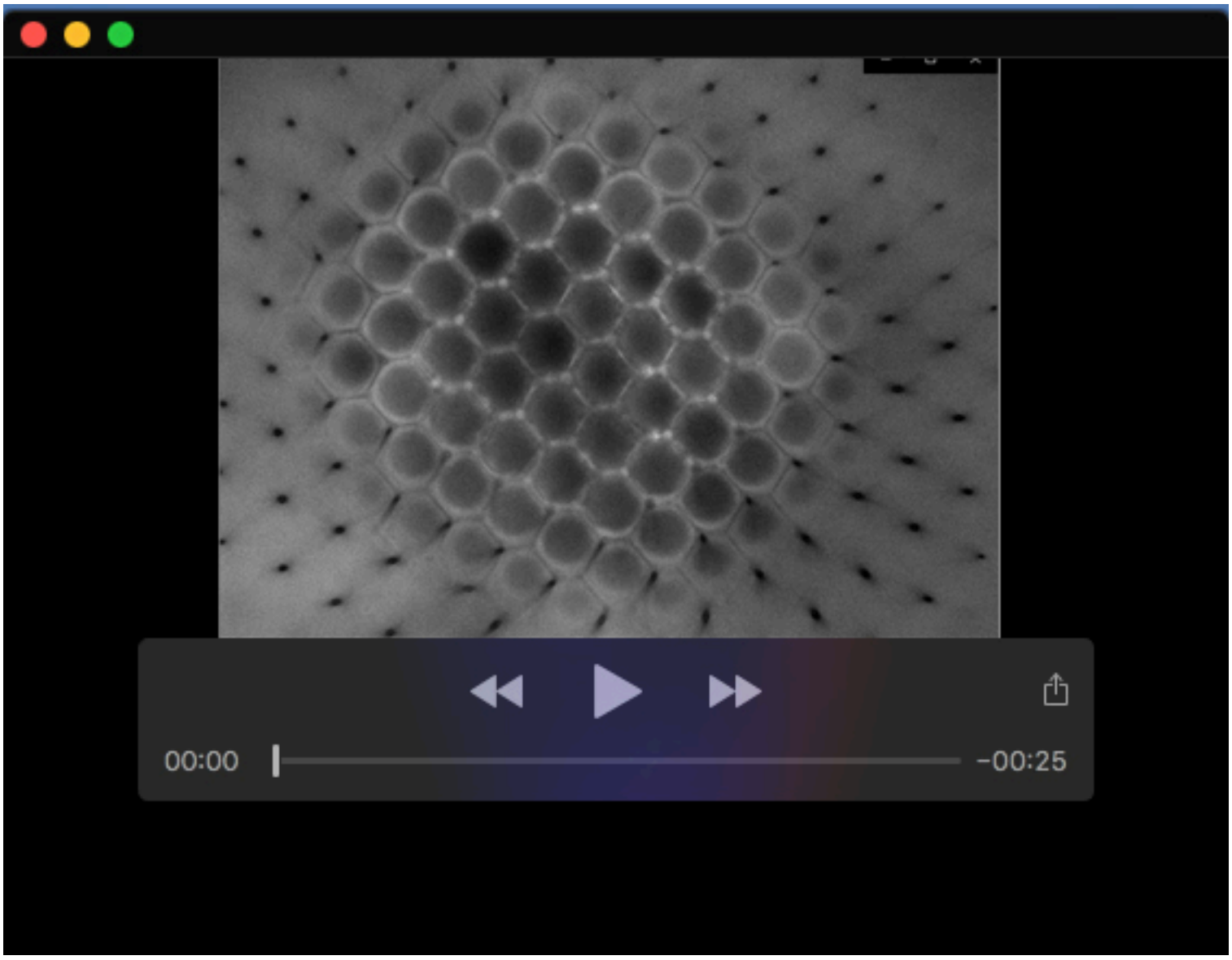

Movie 8. Young *norpA*^{36}*/Y; IGMR>GCaMP6m/+* adult retina at a distal plane (Fig 6).

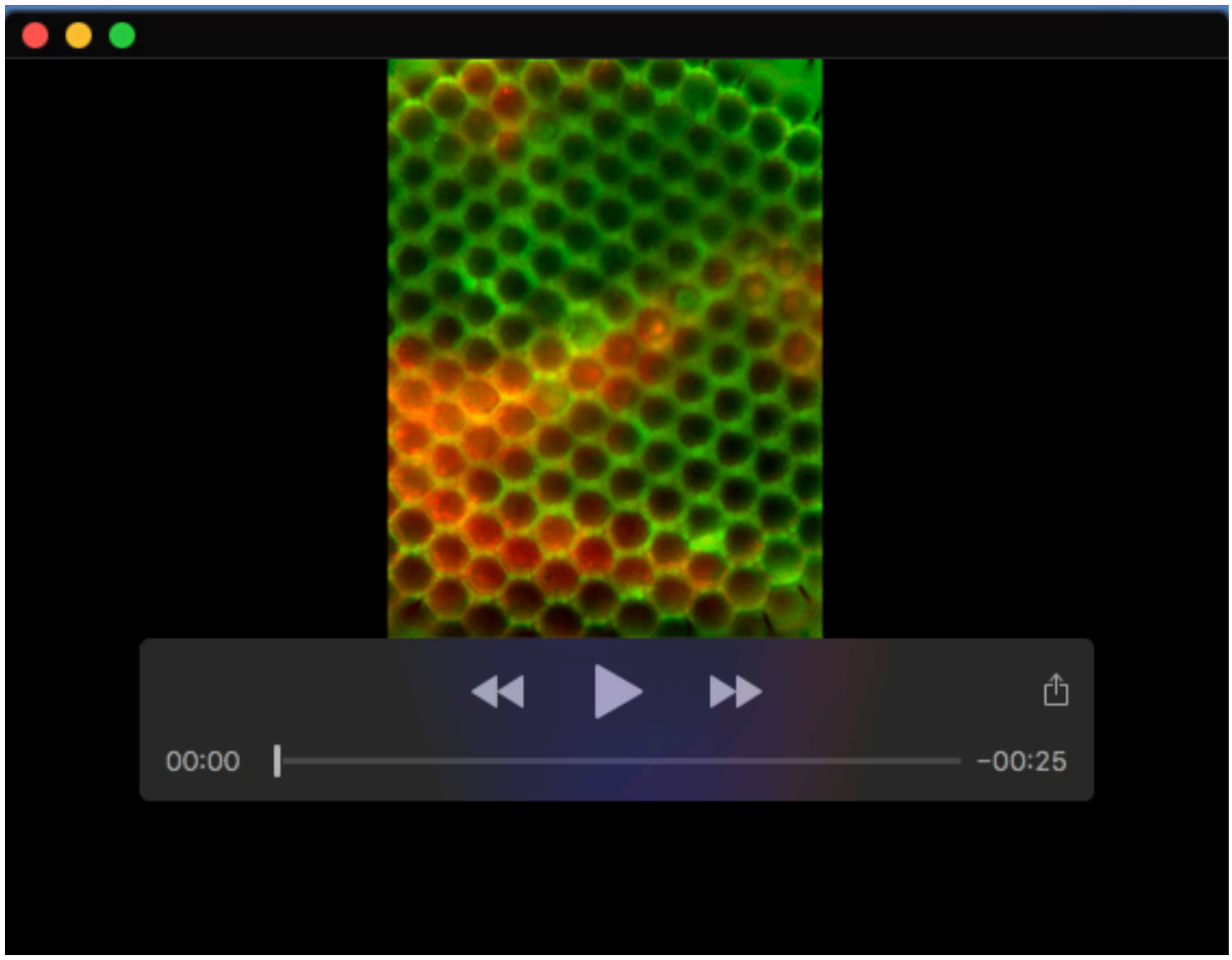

Movie 9. Young *GMR>GCaMP6m/+* adult retina containing *IP3R*$^{-}$ mutant patches (Fig. 6).